Design of a Robot for Transperineal Prostate Needle Placement in MRI Scanner

Gregory S. Fischer[1], Iulian Iordachita[1], Simon P. DiMaio[2], Gabor Fichtinger[1]

[1]*Center for Computer Integrated Surgery*
Johns Hopkins University
Baltimore, MD, gfischer@jhu.edu

[2]*Surgical Planning Lab, Department of Radiology*
Brigham and Women's Hospital, Harvard University
Boston, MA, simond@bwh.harvard.edu

***Abstract*— Numerous studies have demonstrated the efficacy of image-guided needle-based therapy and biopsy in the management of prostate cancer. Magnetic Resonance Imaging (MRI) is an ideal modality for guiding and monitoring prostatic interventions, due to its excellent visualization of the prostate, its sub-structure and surrounding tissues. Despite these advantages, closed high-field MRI scanners (1.5T or greater) have not typically been used in prostate interventions. The strong magnetic field prevents the use of conventional mechatronics and the confined physical space makes it extremely challenging to access the patient. We have designed a robotic assistant system that overcomes these difficulties and promises safe and reliable intraprostatic needle placement inside closed high-field MRI scanners. The paper explains the design process, component selection and the system currently being prototyped.**

I. INTRODUCTION

One out of every 6 men in the United States will be diagnosed with prostate cancer at some point in his life [1]. The definitive method of diagnosis is core needle biopsy and each year approximately 1.5M core needle biopsies are performed, yielding about 220,000 new prostate cancer cases [1]. If the cancer is found to be confined to the prostate, then low-dose-rate permanent brachytherapy–performed by implanting a large number (50-150) of radioactive pellets/seeds into the prostate using thin needles (typically 18G)–is a common treatment option [2]. A complex seed distribution pattern must be achieved with great accuracy in order to eradicate the cancer, while minimizing radiation toxicity to adjacent healthy tissues. There are over 40,000 brachytherapies performed in the U.S. each year and the number is steadily growing [3]. Transrectal Ultrasound (TRUS) is the current "gold standard" for guiding both biopsy and brachytherapy due to its real-time nature, low cost, and apparent ease of use [4]. However, current TRUS-guided biopsy has a detection rate of 20-30% [5], primarily due to the low sensitivity (60%) and poor positive predictive value (25%) of ultrasound [6]. Furthermore, TRUS cannot effectively monitor the implant procedure as implanted seeds cannot be seen in the image. MRI seems to possess many of the capabilities that TRUS is lacking. It has high sensitivity for detecting prostate tumors, high spatial resolution, excellent soft tissue contrast, and multiplanar volumetric imaging capabilities [7]. Closed high-field MRI has not been widely adopted for prostate interventions, because high magnetic field strength and confined physical space present formidable challenges for performing needle placement procedures inside of the imager.

The clinical efficacy of MRI-guided prostate brachytherapy and biopsy was demonstrated by D'Amico, Tempany, et al. at the Brigham and Women's Hospital using a 0.5T open-MRI scanner [8]–[10]. The MR images were used to plan and monitor transperineal needle placement. The needles were inserted manually using a guide comprising a grid of holes, with the patient in the lithotomy position, similarly to the TRUS-guided approach. Zangos et al. used a transgluteal approach with 0.2T MRI, but did not specifically target the tumor foci [11]. Susil et al. described four cases of transperineal prostate biopsy in a closed-bore scanner, where the patient was moved out of the bore for needle insertions and then placed back into the bore to confirm satisfactory placement [12]. Beyersdorff et al. performed targeted transrectal biopsy in a 1.5T MRI unit with a passive articulated needle guide and have reported 12 cases of biopsy to date [13].

Robotic assistance has been investigated for guiding instrument placement in MRI, beginning with neurosurgery [14] and later percutaneous interventions [15], [16]. Chinzei et al. developed a general-purpose robotic assistant for open MRI [17] that was subsequently adapted for transperineal intraprostatic needle placement [18]. Krieger et al. presented a 2-degree of freedom (DOF) passive, unencoded and manually manipulated mechanical linkage to aim a needle guide for transrectal prostate biopsy with MRI guidance [19]. With the use of three active tracking coils, the device is visually servoed into position and then the patient is moved out of the scanner for needle insertion. Other recent developments in MRI-compatible mechanisms include haptic interfaces for fMRI [20] and multi-modality actuators and robotics [21].

This work introduces the design of a novel computer-integrated robotic mechanism for transperineal prostate needle placement in 3T closed-bore MRI. The mechanism is capable of orienting and driving the needle, as well as ejecting radioactive seeds or harvesting tissue samples inside the magnet bore, under remote control of the physician without moving the patient out of the imaging space. This enables the use of real-time multi-modality imaging for precise placement of needles in soft tissues. In addition to structural images, protocols for diffusion imaging and MR spectroscopy will be available intraoperatively, promising enhanced visualization and targeting of pathologies. Accurate and robust needle placement devices, navigated based on such image guidance are becoming invaluable clinical tools and have clear applications in several other organ systems. A description of how this robot fits into the broader complete interventional system is described in [22].

The paper is organized as follows: Section II describes the workspace analysis and design requirements for the proposed device, and Section III details of our prototype design. Preliminary results are presented in Section IV with conclusions in Section V.

1-4244-9713-4/06/$20.00 ©2006 IEEE

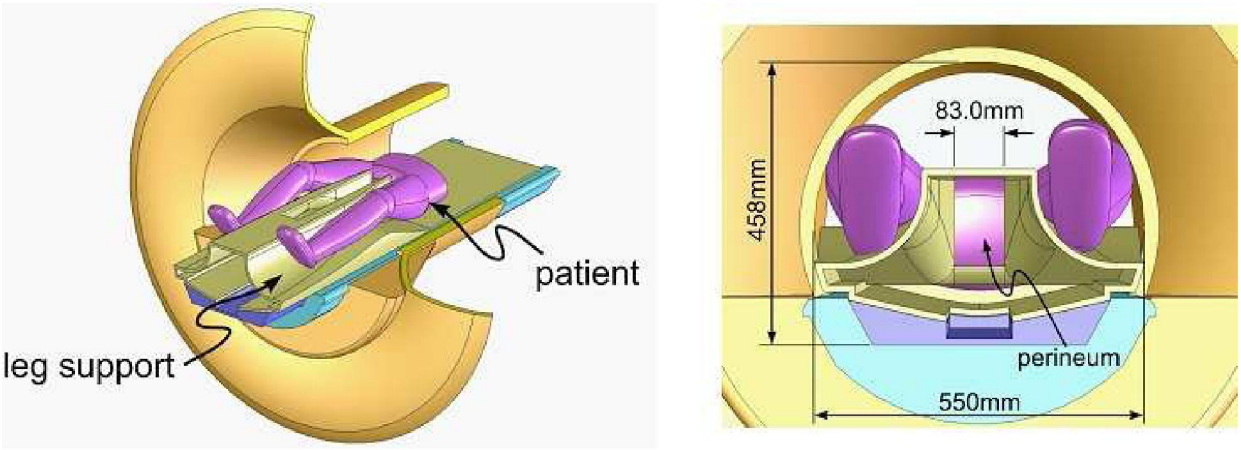

Fig. 1. Patient positioning(left) and workspace available inside leg support / access tunnel(right).

II. Design Requirements

Before designing the surgical robot, we put a great deal of time into determining the detailed technical and clinical specifications. The primary requirements are that the robot is capable of performing the surgical tasks in the entire workspace, and that it does so without interference with the MRI environment, in a safe and predictable manner.

A. Workspace Analysis

The system's primary purpose is to accurately place needles in the prostate with the driving applications being biopsy and brachytherapy seed placement. In our approach, the patient is positioned in the supine position with the legs spread and raised as shown in Fig. 1(left). The patient is positioned in a similar configuration to TRUS-guided brachytherapy, but the MRI bore's constraints require that the legs be spread less and the knees be lower. The robot operates in the confined space between the patient's legs avoiding interference with the patient, MRI scanner components, anesthesia equipment and auxiliary equipment present. This yields a trapezoid-shaped workspace that is tapered toward the patient's perineum. A tunnel-like leg rest, shown in Fig. 1, was designed to fixate the patient in a convenient position and to isolate the robotic manipulator from the patient's body.

The average size of the prostate is 50mm (lateral) × 35mm (anterior-posterior) × 40mm (length). The volume of the prostate volume can be approximated by an elliptical volume formula of the form $V = (.525 \times D_1 \times D_2 \times D_3)$, and the average volume is about 35cc. Due to swelling, the volume of the prostate can enlarge by 25% by the end of the procedure [23]. The standard 60mm x 60mm perineal window of TRUS-guided brachytherapy was increased to 80mm × 100mm, in order to accommodate patient variability and lateral asymmetries in patient setup. In depth, the workspace is extends to 120mm superior of the perineal surface. Direct access to all clinically relevant locations in the prostate is not always possible with a needle inserted purely along apex-base direction due to pubic arch interference. If more than 25% of the prostate diameter is blocked (typically in prostates larger than 55cc), then the patient is usually declined for implantation [23]. Many of these patients will become treatable by introducing two rotational DOF in the sagittal and coronal planes. The resulting workspace overlaid on the leg rest/access tunnel is shown in Fig. 1(right).

B. System Requirements

The workspace analysis allows us to derive the kinematic requirements of the robot. A kinematic diagram is shown in Figure 2, where the primary motions of the base include two prismatic motions and two rotational motions upon a passive linear slide. In addition to these base motions, application-specific motions are also required; these include needle insertion, canula retraction, needle rotation and actuation of the biopsy gun. The accuracy of the individual servo controlled joints is targeted to be 0.1mm, and the needle placement accuracy of the robot is targeted to be better than 1.0mm in free space. The overall system accuracy, however, is expected to be less when effects such as imaging resolution, needle deflection, and tissue deformation are taken into account. The target accuracy is 2mm which approximates the technical accuracy of TRUS-guided procedures and is sufficient to target the minimal clinically significant foci size of 1/2cc [24]. Maximum needle insertion forces were determined to be approximately 15N; with a 100% safety margin, the robot is designed to accommodate twice this force (30N).

The specifications for each motion are shown in Table I. The numbered motions in the table correspond to the labeled joints in the equivalent kinematic diagram shown in Fig. 2. These specifications represent a flexible system that can accommodate a large variety of patients and allow for convenient patient setup. For a proof-of-concept and Phase-1 clinical trials, the two rotational DOF are not required.

C. MRI Compatibility Requirements

A manipulator in an MRI environment cannot employ typical engineering materials and actuators, thus creating a system to operate inside a high-field 1.5−3T MRI scanner adds significant complexity to the design. In order for a device to be MR compatible, it must be MR-safe while not compromising image quality. First, we must avoid the use of ferromagnetic materials because they will cause image artifacts and distortion and can become dangerous projectiles. Second, we must prevent or limit local heating in the proximity of the patient's body; thus the materials and structures used must be either non-conductive or free of loops and eddy currents. Third, we must maintain image quality by limiting the use of conductive materials in the vicinity of the scanner's isocenter. The following section details material and component selection, with the consideration of MR compatibility issues.

TABLE I
KINEMATIC SPECIFICATIONS

	Degree of Freedom	Motion	Requirements
1)	Gross Axial Position	1m	Manual with repeatable stop
2)	Vertical Motion	0-100mm	Precise servo control
3)	Elevation Angle	$+15°$, $-0°$	Precise servo control
4)	Horizontal Motion	$\pm$40mm	Precise servo control
5)	Azimuth Angle	$\pm 15°$	Precise servo control
6)	Needle Insertion	120mm	Cooperative or Automated
7)	Canula Retraction	60mm	Cooperative or Automated
8)	Needle Rotation	360°	Manual or Automated

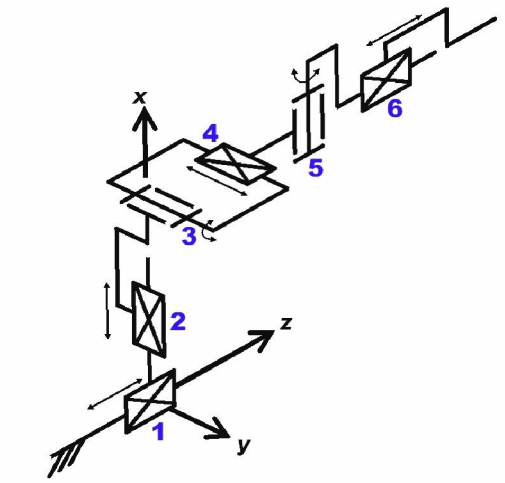

Fig. 2. Equivalent kinematic diagram of the robot. Details the required six degrees of freedom for needle insertion procedures with this manipulator.

III. SYSTEM AND COMPONENT DESIGN

A. Overview

The development of the robot will take place in several phases, through an evolution of prototypes. The first embodiment will have the vertical and horizontal motions actuated; this yields a high-resolution needle guide functionally similar to the template in conventional brachytherapy. This initial prototype can be rapidly fabricated by laser-cutting the links out of acrylic sheets. The base of the robot will also be made of Polyetherimide (Ultem) and Polycarbonate (Lexan), and will be mounted on an aluminum linear guide with plastic bushing elements made by Igus[1]. The slide allows manual placement of the robot in its end position inside of the leg rest/tunnel with a positive locking mechanism that ensures a reliable, repeatable placement with respect to the scanner's coordinate system. The robot can be manually translated to the foot of the bed to reload brachytherapy needles or remove the biopsy sample or for a rapid removal of the entire robot in case of emergency. A similar, but much smaller linear guide from Igus is to be used as a base for the mechanisms, as shown in the final design shown in in Fig. 8. The purpose of this simplified 2-DOF design is to validate that the robot: a) has the desired workspace, b) functions properly in a 3T field, c) does not cause prohibitive imaging artifacts and distortion and d) yields sufficient accuracy in joint motion and overall needle placement.

The next design iteration will produce a 4-DOF robot base with the links made out of high strength, dimensionally stable, highly electrically insulating and sterilizable plastic (e.g. Ultem or PEEK). The 4-DOF base has a modular platform that allows for different end effectors to be mounted on it. The two initial end effectors will accommodate biopsy guns and brachytherapy needles. Both require an insertion phase, and the latter requires an additional controlled linear motion to accommodate cannula retraction to release the brachytherapy seeds. Detailed design of the end effectors is not presented here; they are to be based on pneumatically actuated liner guides. Sterility is also an issue in medical robots, and that is being taken into consideration for the design of the end effectors. In particular, the portions of the manipulator that come in direct contact with the patient and/or the needle will be removable and disposable or sterilizable. The remainder of the robot can be draped.

B. Mechanism Design

Mechanism design is particularly important to maintain a rigid, compact profile. Based upon analysis of the workspace and the application, the following additional design requirements have been adopted:

1) Linear motion should be able to be decoupled from the rotations since the majority of procedures will not require the two rotational DOF.
2) Actuator motion should be in the axial direction (aligned with B_o field) to maintain a compact profile.
3) Extension in both the vertical and horizontal planes should be telescopic to avoid linear guides that may prevent the robot from fitting in the constrained workspace.

The four primary base DOF (Motions 2−5 in Table I) are broken into two decoupled 2-DOF planar motions. In order to maintain high rigidity, a planar bar mechanism are used. Motion in the vertical plane includes 100mm of vertical travel, and up to 10° of positive elevation angle. This is achieved using a modified version of a scissor lift mechanism that is traditionally used for plane parallel motion. By coupling two such mechanisms as shown in Fig. 3, 2-DOF can be achieved. Stability is increased by using a pair of such mechanisms in the rear. For prismatic motion alone, both slides are moved together. To tilt the surface, the front slide is fixed and the rear is moved relative to it. To aid in decoupling the motion, the actuator for the rear slide is fixed to the carriage of the primary motion linear drive.

Motion in the horizontal plane is accomplished with a second planar bar mechanism. This motion is achieved by coupling two straight line motion mechanisms as shown in Fig. 4, generally referred to as Scott-Russell mechanisms[2]. By combining two straight-line motions, both prismatic and rotational motions can be realized in the horizontal plane. Actuation is provided by a modified compact pneumatic cylinder that is oriented in the axial direction. Fig. 4 shows the system in the 1-DOF configuration where only translation is available. This is accomplished by linking the front and rear mechanisms with a connecting bar; it is straightforward to add the rotational motion for future designs by replacing the rigid connecting bar with a pneumatic cylinder or by actuating the rear mechanism in a similar fashion as the front.

[1]Igus NK02 linear guide

[2]Mechanism designs - http://www.brockeng.com/mechanism

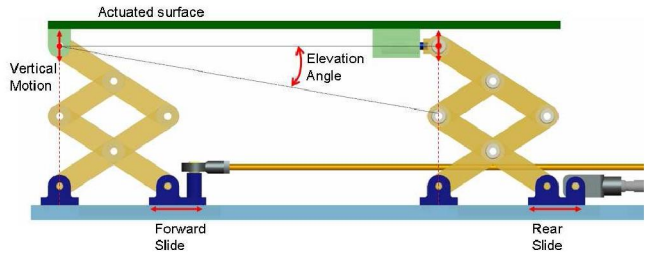

Fig. 3. Mechanism design for motion in the vertical plane. Coupling the forward and rear motion provides for vertical travel, independently moving the rear provides for elevation angle adjustment.

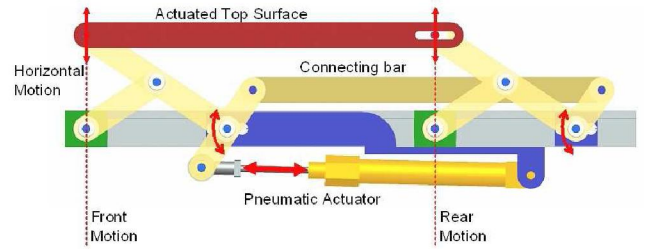

Fig. 4. Mechanism design for motion in the horizontal plane. Provides for plane parallel motion, can provide both translation and rotation by actuating rear motion independently.

C. Actuator Design

Many robots use electro-dynamic actuation, however, the very nature of an electric motor precludes its use in high-field magnetic environments. Therefore, it is necessary to use actuators that are compatible with the MR environment, or to use a transmission to mechanically couple the manipulator in the MRI scanner to standard actuators situated outside the high field. The latter can take the form of flexible drivehafts [19], push-pull cables or hydraulic (or pneumatic) couplings [20].

To maintain actuators in close proximity to the robot, an alternative to electric motors is hydraulic or pneumatic actuators. Hydraulic actuators offer the advantages of high stiffness and near-incompressible flow at the expense of speed/bandwidth, inconvenient fluid connections when a permanently closed system is not possible and the potential for leaks. Pneumatic actuators offer relatively high speed, large power density and availability and cost effectiveness of components, at the expense of decreased stiffness and less straightforward control due to nonlinearities including the compressibility of air and relatively large friction forces. We chose to use pneumatic actuators for the robot.

Valves are necessary to manipulate a pneumatic actuator. There are essentially three basic types of valves that are used for servo control of a pneumatic cylinder:

1) High-bandwidth on-off valves used for PWM control
2) Spool valves for proportional air flow rate control
3) Pressure regulators for differential air pressure control

Typical pneumatic valves are operated directly by a solenoid coil or indirectly by a small pilot valve that is actuated by a solenoid coil. Unfortunately, as with electric motors, the very nature of a solenoid coil is a contraindication for its use in an MR environment. Therefore, it is imperative to find a suitable way to actuate these valves. A solution lies in piezoelectric actuation that can be used to control the valves or the valves' pilots. Such valves can either be custom-made by replacing the solenoid unit of a standard valve with a piezoelectric actuator, or they can be purchased as standard parts from select companies.

D. Position Sensing

The remaining component of the actuator system is the sensing element. Standard methods of position sensing that are suitable for pneumatic cylinders include: linear potentiometers, linear variable differential transformers (LVDT), capacitive sensors, ultrasonic sensors, magnetic sensors, laser sensors, optical encoders, and cameras (machine vision). Most of these sensing modalities are not practical for use in an MR environment. However, there are two methods that do appear to have potential: 1) linear optical encoders and 2) direct MRI image guidance.

Standard optical encoders[3] have been tested in a 3T MRI scanner for functionality and in a 1.5T scanner for induced effects in the form of imaging artifacts. Examining the test results shown in Fig. 5, it appears that beyond 50mm from the encoder (positioned at the isocenter on top of a cylindrical phantom), there is little or no induced artifact when imaged in a GE Signa Excite 1.5T scanner. This is very promising because the design can be made such that the sensing elements are sufficiently far from the scanner isocenter. If initial trials demonstrate a problem with these sensors, commercially available fiber optic encoders or non-magnetic laser encoders may be adapted to work in an MR environment.

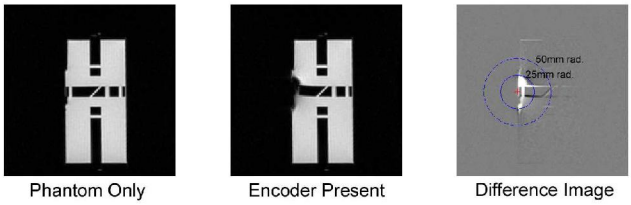

Fig. 5. MR compatibility trial of optical encoder in a 1.5T scanner.

Direct MRI-based image guidance shows great promise for high-level control, safety and verification, and for robot-scanner registration; however, the refresh rate and resolution is probably not sufficient for use in low-level servo control of a robot joint. Practical methods of robot tracking are discussed in [19]; the most applicable for high-level control of the robot being the use of active tracking coils to determine robot configuration and needle location with respect to the scanner and image coordinate systems.

E. Robot Control

Low-level control of pneumatic pistons can be achieved using actuation techniques related to the valve types listed in Section III-C. It is the authors' intention to test each of them and determine the pros and cons of each. Pulse width modulation (PWM) control requires a fast-acting 5/3 valve or pair of 3/2 valves which are generally the lowest cost of the valve types, and only require digital outputs on the controller. However these advantages probably do not outweigh the decreased stability and jitter that may arise and are totaly unacceptable for a medical robot.

A common method of servo control of pneumatic pistons is based on the use of proportional flow valves; usually spool valves that modulate the air flow between two outputs

[3]US Digital EM1-0-500 encoder module with PC5 differential line driver

corresponding to the two sides of the cylinder being controlled. The primary advantage of proportional flow valves is the capability of smooth, high-bandwidth control of the cylinder.

A pneumatic control modality that does not appear to have been as widely discussed in the position control literature is based on the use of proportional pressure regulators. The pressure on both sides of the cylinder's piston can be maintained and modulated as necessary to move the shaft, allowing faster actuation and potentially a stiffer system. Further, piezoelectrically actuated proportional pressure regulators that contain no ferromagnetic material are available off the shelf. The downside to this scheme is cost; it is necessary to have two pressure regulators per actuator, each with its own analog control signal. The test fixture shown in Fig. 6 is used for evaluating the valve types and control methods. It consists of a regulator/filter, an accumulator/distribution block, a proportional flow spool valve (to be substituted with the appropriate type for each trial), a pneumatic cylinder and a linear optical encoder.

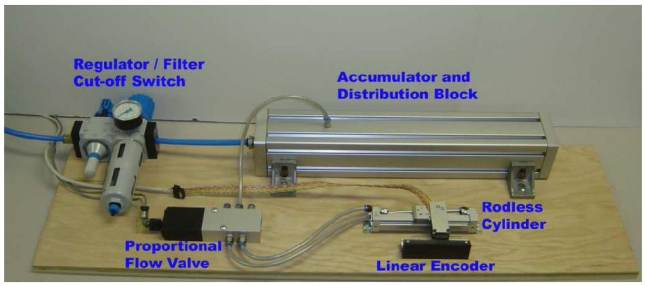

Fig. 6. Test fixture for pneumatic servo control.

At present, our first choice for valves is a pair of proportional pressure regulators. Piezoelectrically actuated proportional air pressure valves that appear to be perfectly suited for the task are available from Hoerbiger-Origa[4]. The valves will be in an enclosure situated near the foot of the scanner bed; this is a compromise between proximity of controls to the MRI scanner and length of tubing between the valves and the actuators.

F. Controller Interface

Low level control software will be implemented on an embedded PC-104 computer using the Real Time Application Interface (RTAI)[5] Linux kernel extension to allow for the accurate clock necessary for PC-based servo control. A PC-104 analog output module will be used to control the valves (two outputs per axis) and an analog input module will be used to monitor pressure sensors on each valve output. An FPGA module will be used for monitoring the incremental linear optical encoders on each joint including the index pulse which will be used for homing the system; it will also provide digital I/O for limit switches and brakes. The PC-104 computer stack, DC-DC power regulator, valves, and pressure sensors will be located in an RF-shielded enclosure located in the scanner room near the foot of the scanner bed (about 2m from the bore). Pneumatic connections from the controller enclosure to the manipulator that is sitting on the bed in the scanner bore will be simplified with a multi-port pneumatic connector and bundled air tubing.Connections into and out of the scanner room only include a regulated compressed air supply and a fiber optic ethernet connection. High level control an visualization is situated on an RTAI Linux-based laptop PC sitting in the MR console room connected through the fiber optic ethernet link. An overview of the connections and breakdown of component locations is shown in Fig. 7.

Interface with the robot will be via a 3D Slicer-based[6] software GUI running on the laptop PC in the scanner's console room. The laptop runs a DICOM server to retrieve images from the scanner console. Both preoperative and intra-operative images can be loaded into the application for procedure planning and for intra-operative guidance. For early iterations of the system, a target and entry point will be chosen on the control PC, and the robot will align the needle guide appropriately. The needle will be inserted either entirely manually or under cooperative control where an encoded slider will be manipulated by the clinician, while the robotic insertion follows. Keeping a human in the loop increases the safety and allows for live MRI images to help monitor progress. If haptic feedback is deemed necessary, force sensing can be incorporated into the needle driver and a standard impedance controlled master will be used in the console room in place of the encoded slider. In the future, visual servoing of the robot and bevel-based steering of the needle [26], as well as automated insertion, can be implemented.

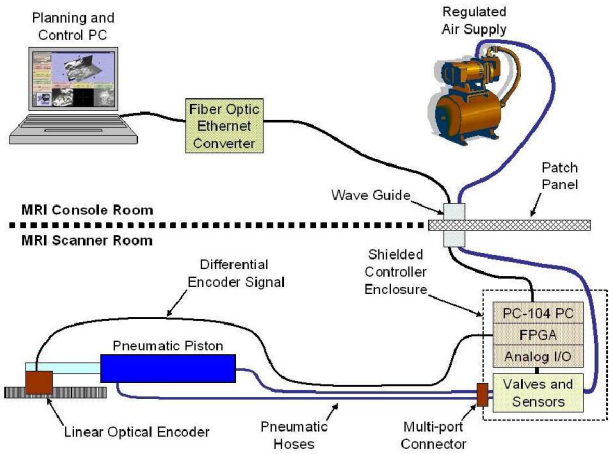

Fig. 7. Controller connection diagram shown with a single representative actuator. High level control and visualization take place outside of the scanner room. The low level joint controller and valves are placed in the scanner room at the foot of the bed; actuators and encoders are in the scanner bore.

IV. Results

Design and analysis are complete, material selection has been finalized and the controller selected. The robot is in the process of being constructed. The controller has been configured and is being programmed. Initial trials with pneumatic cylinder control with proportional valves have begun and are successful thus far; a rigorous comparison of control algorithms will be undertaken in the near future. The trials are being performed using the test fixture shown in Fig. 6. Initial trials with some materials (including aluminum and plastics) and sensors (including optical encoders) in the MRI scanner have proved successful as well.

Incorporating all of the discussed specification, designs, and design limitations, the design of the robot is as shown in Fig.

[4]Hoerbiger-Origa PRE-U piezo valve
[5]RTAI - http://www.rtai.org
[6]3D Slicer - http://www.slicer.org

8. It is conceivable that the robot takes a change of form after initial prototypes are built and tested. The immediate target is to implement a 2-DOF prismatic base in the context of an MRI scanner and leg rest/tunnel, in the actual workspace. Thus far, a 1-DOF version has been constructed as shown in Fig. 9. It is being used for initial accuracy and MR compatibility validation experiments .

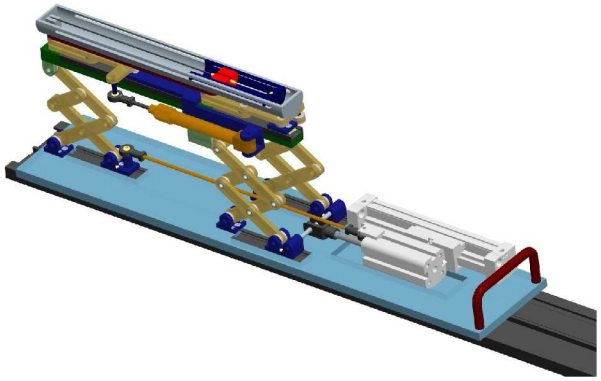

Fig. 8. Complete robot mechanism design. Shown on manual gross positioning slide with brachytherapy end effector.

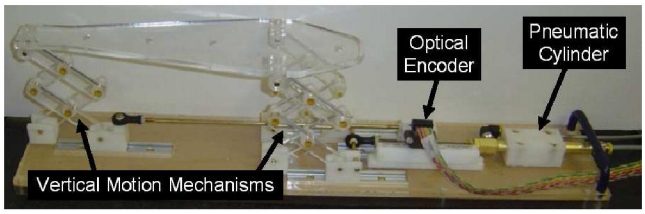

Fig. 9. Preliminary 1-DOF robot base prototype for validation experiments.

V. Conclusion

We have designed an MR-compatible manipulator that can be used for needle placement in the prostate for biopsy and brachytherapy procedures. The robot has been designed such that it will operate in the confined space between the patient's legs inside a leg rest/tunnel in a high-field closed bore MRI scanner. The initial application will be prostate biopsy, followed later by brachytherapy seed placement. The design of the manipulator allows for treatment of patients that may have otherwise been denied such treatment because of contraindications such as significant pubic arch interference. We will deploy a platform not only for prostate biopsy and brachytherapy, but also for injections, thermal ablation, and optical sensing modalities under MR image guidance. The ultimate goal of the system is to have a robot capable of accurately and efficiently performing needle placement procedures in the prostate under real-time MRI image guidance.

References

[1] A. Jemal, "Cancer statistics, 2004," in *CA Cancer J Clin*, vol. 54(8), 2004.

[2] J. Blasko, T. Mate, J. Sylvester, P. Grimm, and W. Cavanagh, "Brachytherapy for carcinoma of the prostate: techniques, patient selection, and clinical outcomes," in *Semin Radiat Oncol*, vol. 12(1), pp. 81–94, 2002.

[3] M. Cooperberg, D. Lubeck, M. Meng, S. Mehta, and P. Carroll, "The changing face of low-risk prostate cancer: trends in clinical presentation and primary management," in *J Clin Oncol*, vol. 22(11), pp. 2141–9, 2004.

[4] J. P. Jr., "Prostate cancer: assessment of risk using digital rectal examination, tumor grade, prostate-specific antigen, and systematic biopsy," in *Radiol Clin North Am*, vol. 38(1), pp. 49–58, 2000.

[5] M. Terris, E. Wallen, and T. Stamey, "Comparison of mid-lobe versus lateral systematic sextant biopsies in detection of prostate cancer," in *Urol Int*, vol. 59, pp. 239–242, 1997.

[6] D. Keetch, J. McMurtry, D. Smith, G. Andriole, and W. Catalona, "Prostate specific antigen density versus prostate specific antigen slope as predictors of prostate cancer in men with initially negative prostatic biopsies," in *J Urol*, vol. 156(2 Pt 1), pp. 428–31, 1996.

[7] K. Yu and H. Hricak, "Imaging prostate cancer," in *Radiol Clin North Am*, vol. 38(1), pp. 59–85, 2000.

[8] V. D'Amico, R. Cormack, C. Tempany, S. Kumar, G. Topulos, H. Kooy, and C. Coleman, "Real-time magnetic resonance image-guided interstitial brachytherapy in the treatment of select patients with clinically localized prostate cancer," in *International Journal of Radiation Oncology*, vol. 42, pp. 507–515, Oct. 1998.

[9] A. D'Amico, C. Tempany, R. Cormack, N. Hata, M. Jinzaki, K. Tuncali, M. Weinstein, and J. Richie, "Transperineal magnetic resonance image guided prostate biopsy," in *J Urol*, vol. 164(2), pp. 385–7, 2000.

[10] M. So, S. Haker, K. Zou, A. S. Barnes, R. Cormack, J. Richie, A. D'Amico, and C. Tempany, "Clinical Evaluation of MR-guided Prostate Biopsy," in *ISMRM 13th Scientific Meeting and Exhibition*, 2005.

[11] S. Zangos, K. Eichler, K. Engelmann, M. Ahmed, S. Dettmer, C. Herzog, W. Pegios, A. Wetter, T. Lehnert, M. Mack, and T. J. Vogl, "MR-guided transgluteal biopsies with an open low-field system in patients with clinically suspected prostate cancer: technique and preliminary results," in *Eur Radiol*, vol. 15(1), pp. 174–82, 2005.

[12] R. Susil, K. Camphausen, P. Choyke, E. R. McVeigh, G. Gustafson, H. Ning, R. Miller, E. Atalar, C. Coleman, and C. Ménard, "System for prostate brachytherapy and biopsy in a standard 1.5 T MRI scanner," in *Magnetic Resonance in Medicine*, vol. 52, pp. 683–687, 2004.

[13] D. Beyersdorff, A. Winkel, B. Hamm, S. Lenk, S. Loening, and M. Taupitz, "MR imaging-guided prostate biopsy with a closed MR unit at 1.5 T: initial results," in *Radiology*, vol. 234(2), pp. 576–581, 2005.

[14] K. Masamune, E. Kobayashi, Y. Masutani, M. Suzuki, T. Dohi, H. Iseki, and K. Takakura, "Development of an MRI-compatible needle insertion manipulator for stereotactic neurosurgery," in *J Image Guid Surg*, vol. 1(4), pp. 242–8, 1995.

[15] A. Felden, J. Vagner, A. Hinz, H. Fischer, S. Pfleiderer, J. Reichenbach, and W. Kaiser, "ROBITOM-robot for biopsy and therapy of the mamma," in *Biomed Tech (Berl)*, vol. 47 Suppl 1 Pt 1, pp. 2–5, 2002.

[16] E. Hempel, H. Fischer, L. Gumb, T. Hohn, H. Krause, U. Voges, H. Breitwieser, B. Gutmann, J. Durke, M. Bock, and A. Melzer, "An MRI-compatible surgical robot for precise radiological interventions," in *Computer Aided Surgery*, pp. 180–191, Apr. 2003.

[17] K. Chinzei, N. Hata, F. Jolesz, and R. Kikinis, "MR compatible surgical assist robot: system integration and preliminary feasibility study," in *Medical Image Computing and Computer Assisted Intervention*, vol. 1935, pp. 921–933, Oct. 2000.

[18] S. DiMaio, S. Pieper, K. Chinzei, G. Fichtinger, C. Tempany, and R. Kikinis, "Robot assisted percutaneous intervention in open-MRI," in 5^{th} *Interventional MRI Symposium*, p. 155, 2004.

[19] A. Krieger, R. Susil, C. Menard, J. Coleman, G. Fichtinger, E. Atalar, and L. Whitcomb, "Design of a novel MRI compatible manipulator for image guided prostate interventions," in *IEEE Transactions on Biomedical Engineering*, vol. 52, pp. 306–313, Feb. 2005.

[20] G. Ganesh, R. Gassert, E. Burdet, and H. Bleule, "Dynamics and control of an MRI compatible master-slave system with hydrostatic transmission," in *International Confennee on Robotics and Automation*, pp. 1288–1294, Apr. 2004.

[21] D. Stoianovici, "Multi-imager compatible actuation principles in surgical robotics," in *International Journal of Medical Robotics and Computer Assisted Surgery*, vol. 1, pp. 86–100, 2005.

[22] S. DiMaio, G. Fischer, S. Haker, N. Hata, I. Iordachita, C. Tempany, and G. Fichtinger, "System for MRI-guided Prostate Interventions," in *IEEE International Conference on Biomedical Robotics and Biomechatronics*, Feb. 2006.

[23] K. Wallner, J. Blasko, and M. Dattoli, *Prostate Brachytherapy Made Complicated, 2nd Ed.* SmartMedicine Press, 2001.

[24] J. Bak, S. Landas, and G. Haas, "Characterization of prostate cancer missed by sextant biopsy," in *Clin Prostate Cancer*, vol. 2(2), pp. 115–118, Sept. 2003.

[25] A. Kapoor, N. Simaan, and P. Kazanzides, "A system for speed and torque control of DC motors with application to small snake robots," in *Mechatronics and Robotics*, 2004.

[26] R. Webster III, J. Memisevic, and A. Okamura, "Design Considerations for Robotic Needle Steering," in *IEEE International Conference on Robotics and Automation*, pp. 3599–3605, 2005.